PHYSICAL REVIEW B **76**, 060402(R) (2007)

Incommensurate magnetic structure in the orthorhombic perovskite $ErMnO_3$

F. Ye,[1,*] B. Lorenz,[2] Q. Huang,[3] Y. Q. Wang,[2] Y. Y. Sun,[2] C. W. Chu,[2] J. A. Fernandez-Baca,[1] Pengcheng Dai,[4,1] and H. A. Mook[1]

[1]*Neutron Scattering Science Division, Oak Ridge National Laboratory, Oak Ridge, Tennessee 37831-6393, USA*

[2]*Department of Physics and TCSUH, University of Houston, Houston, Texas 77204-5002, USA*

[3]*NIST Center for Neutron Research, National Institute of Standards and Technology, Gaithersburg, Maryland 20899, USA*

[4]*Department of Physics and Astronomy, The University of Tennessee, Knoxville, Tennessee 37996-1200, USA*

(Received 18 May 2007; revised manuscript received 2 July 2007; published 2 August 2007)

By combining dielectric, specific heat, and magnetization measurements and high-resolution neutron powder diffraction, we have investigated the thermodynamic and magnetic and structural properties of the metastable orthorhombic perovskite $ErMnO_3$ prepared by high-pressure synthesis. The system becomes antiferromagnetically correlated below 42 K and undergoes a lock-in transition at 28 K with propagation wave vector $(0,k_b,0)$, which remains incommensurate at low temperature. The intercorrelation between the magnetic structure and electric properties and the role of the rare earth moment are discussed.

DOI: 10.1103/PhysRevB.76.060402 PACS number(s): 75.47.Lx, 75.30.Kz, 75.50.Ee, 75.25.+z

Multiferroic materials (in which magnetism and ferroelectricity coexist) have attracted great attention in recent years because of their fundamental as well as technical importance.[1–6] Among these, the frustrated magnets are considered the most promising candidates to achieve mutual control of magnetic and ferroelectric properties. For example, the rare-earth perovskite manganites $RMnO_3$ (R=Tb, Dy) exhibit flopping of the electric polarization (P) with applied magnetic field H, or reversal of the magnetic helicity by electric field E.[1,7] Despite the continuing discovery of new multiferroic materials, the understanding of the fundamental mechanism of the magnetic-ferroelectric coupling is far from completed and remains a challenge.[8–10] One possible microscopic mechanism of ferroelectricity (FE) induced by the complex magnetic order involves a noncollinear coupling between a uniform electric polarization P to an inhomogeneous magnetic order M. The symmetry-allowed term $PM\partial M$ breaks the space inversion symmetry and gives rise to electric polarization as soon as magnetic ordering of a proper kind sets in. Generally speaking, a spiral or helical magnetic structure in frustrated magnets with appropriate crystal symmetry leads to an electric polar state.[11–13]

However, the spiral magnetic structure is not the only source of FE. It was proposed that a collinear E-type magnetic structure in the orthorhombic perovskite manganites and nickelates allows a finite ferroelectric polarization.[14] The estimated P might be orders of magnitude larger than that in the helical magnets, because the underlying mechanism does not involve spin-orbit interactions or noncollinear spin structures. Instead, it is the competition between the elastic energy and the energy gain due to the virtual hopping of e_g electrons within the zigzag spin chains that causes the coherent displacement of the oxygen atoms in the ground state. Indeed, giant magnetoelectric response and spontaneous electric polarization have been reported in the orthorhombic $HoMnO_3$ and $YMnO_3$ manganites, in which the FE is established simultaneously with the collinear magnetic structure.[15,16] Furthermore, there is considerable enhancement of electric polarization P in $HoMnO_3$ when the holmium ions order below 15 K, strongly suggesting the involvement of the rare-earth moment.[16] To extend our search for possible FE materials as well as to assess the role of the rare-earth moment in stabilizing the FE, we have prepared orthorhombic perovskite $ErMnO_3$ manganite where the Er^{3+} moment orders at much lower temperature. We find that the low-T magnetic structure of orthorhombic $ErMnO_3$ is incommensurate (ICM), in contrast to the generally accepted E-type phase for this distorted manganite.[17,18] Antiferromagnetic fluctuation sets in at $T_{N1}\approx 42$ K with wave vector of $(0,k_b,0)$. The wave vector locks onto a fixed value of $q_m=(0,0.433,0)$ below $T_{N2}\approx 28$ K. Even at the lowest temperature, the magnetic order remains short range. Consistent with this, the FE in $ErMnO_3$ is relatively weak compared to $HoMnO_3$ and $YMnO_3$. This highlights the close connection between the emergence of ferroelectricity and the long-range magnetic structure.

The powder specimens of $ErMnO_3$ were prepared using solid-state reaction methods.[15] The hexagonal compounds were transformed into the orthorhombic structure by high-pressure sintering for 5 h (1100 °C, 3.5 GPa). The specific heat and dielectric properties were measured employing a physical property measurement system (Quantum Design) for temperature control, using the heat capacity option as well as a homemade capacitance probe adapted to the cryostat, respectively. For dielectric measurements, the sample was shaped as a parallel plate capacitor and silver paint was used as electrodes. Magnetic properties were measured in a magnetic property measurement system (Quantum Design). Neutron powder diffraction (NPD) patterns were collected on the high-resolution, 32-counter BT-1 diffractometer and BT-7 triple-axis spectrometer at the NIST Center for Neutron Research (NCNR). A total mass of 1.5 g was used for the NPD measurement.

Figures 1(a)–1(c) display the temperature dependence of the dielectric constant $\varepsilon(T)$, magnetization $M(T)$, and the specific heat $C_p(T)$ of the orthorhombic $ErMnO_3$. Below the Néel temperature, $\varepsilon(T)$ increases rapidly and passes through a broad maximum at low T. Two transitions are clearly seen in the temperature derivative $d\varepsilon(T)/dT$, where T_{N1} is well defined at 42 K and a second transition takes place near 30 K with strong hysteresis, indicating its first-order charac-

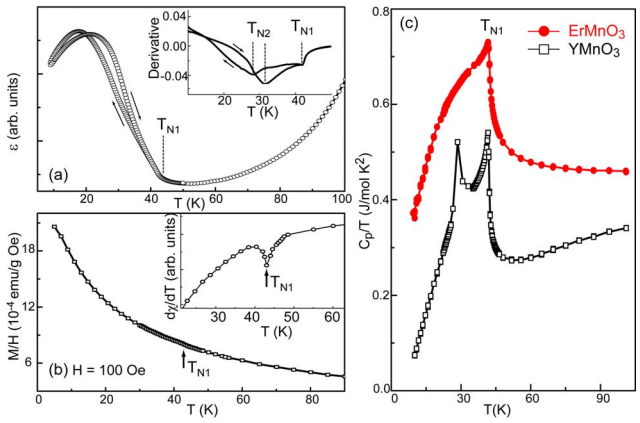

FIG. 1. (Color online) Temperature dependence of (a) the dielectric constant $\varepsilon(T)$, (b) the magnetization $M(T)$, and (c) the specific heat $C_p(T)$ of the orthorhombic $ErMnO_3$. Inset shows the T derivative of $\varepsilon(T)$ in the lower temperature range. $C_p(T)$ data for the orthorhombic $YMnO_3$ (similar to the work reported by Kim *et al.* 19) are also plotted for comparison.

ter. Similarly, $M(T)$ shows a small anomaly at T_{N1}, while that transition can be better seen in $d\chi/dT$. The signals of $M(T)$ at lower temperatures are dominated by the paramagnetic moment from the rare-earth erbium ions. Figure 1(c) compares the specific heat $C_p(T)$ of $ErMnO_3$ with that of the orthorhombic $YMnO_3$ in which spontaneous electric polarizations occurs.[16] While $C_p(T)$ of $YMnO_3$ shows two sharp peaks which correspond to the onset of antiferromagnetic (AFM) correlations and a lock-in transition to long-range magnetic order with the onset of ferroelectricity,[16,19,20] the $C_p(T)$ of $ErMnO_3$ only displays a sharp peak near 42 K; the second transition near T_{N2} is less discernible.

TABLE I. Structural parameters of orthorhombic $ErMnO_3$ from Rietveld refinement at 3.6, 55, and 300 K. Atomic positions [Er $4b(x,y,0.25)$, Mn $4c(0.5,0,0)$, O_1 $4c(x,y,0.25)$, O_2 $8d(x,y,z)$]. R_p is the residual, and R_{wp} is the weighted residual. The temperature factor U_{iso} of Mn is fixed in the refinement.

S.G.	3.6 K *Pbnm*	55 K *Pbnm*	300 K *Pbnm*
a (Å)	5.2273(2)	5.2270 (2)	5.2315 (3)
b (Å)	5.7922(2)	5.7926 (2)	5.7987 (4)
c (Å)	7.3277(3)	7.3308 (3)	7.3410 (4)
V (Å^3)	221.865 (12)	221.960 (11)	222.699 (31)
Mn U_{iso} (Å^2)	0.0030	0.0030	0.0030
Er x	−0.0171(9)	−0.0174(9)	−0.0188(10)
y	0.0840 (7)	0.0846 (7)	0.0844 (7)
U_{iso} (Å^2)	0.0038 (14)	0.0044 (13)	0.0043 (10)
O_1 x	0.113 (1)	0.113 (1)	0.113 (1)
y	0.461 (1)	0.462 (1)	0.462 (1)
U_{iso} (Å^2)	0.0019 (12)	0.0018 (11)	0.0058 (8)
O_2 x	0.6984 (8)	0.6989 (7)	0.7000 (8)
y	0.3268 (7)	0.3278 (7)	0.3266 (8)
z	0.0541 (6)	0.0555 (6)	0.0536 (6)
U_{iso} (Å^2)	0.0019 (12)	0.0018 (11)	0.0058 (8)
Mn-O_1-Mn (deg)	141.2 (4)	142.1 (3)	142.0 (3)
Mn-O_2-Mn (deg)	143.7 (3)	143.2 (2)	144.0 (2)
R_p (R_{wp}) (%)	7.13 (8.90)	6.55 (8.27)	6.70 (8.39)
χ^2	0.91	0.81	0.82

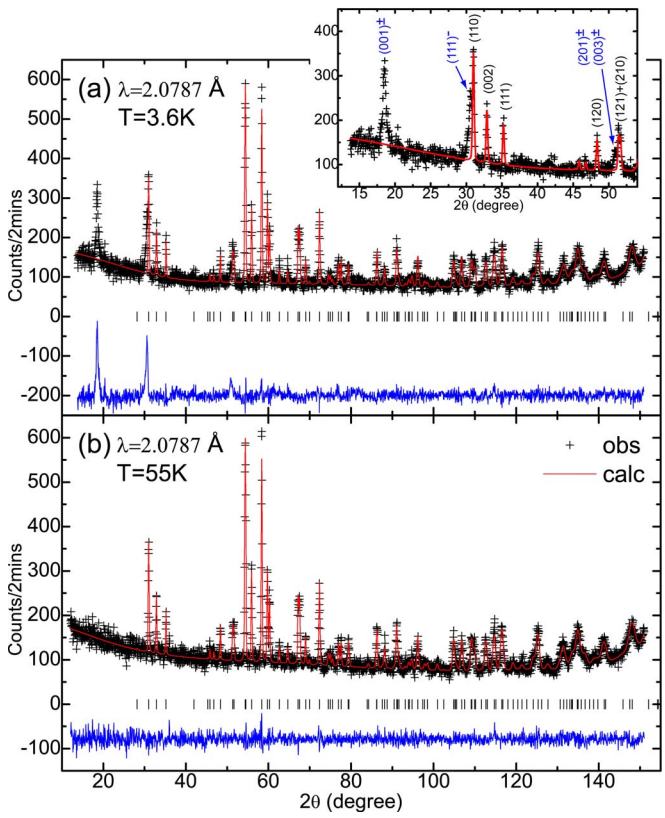

FIG. 2. (Color online) (a) High-resolution neutron powder diffraction pattern of the orthorhombic $ErMnO_3$ specimen at (a) 3.6 K (below T_{N1}) and (b) 55 K (above T_{N1}). Inset zooms in on the lower-angle portion of the diffraction pattern, with the magnetic and structural reflections indexed.

To determine the magnetic structure and its correlation with the bulk measurement results, we performed NPD at a series of temperatures near the transition and at room temperature with incident neutron wavelength $\lambda = 2.0787$ Å. The nuclear structure peaks can be described by a single phase with space group *Pbnm* at all temperatures. No hexagonal phase could be detected within the experimental error. Figures 2(a) and 2(b) plot the representative diffraction profiles at 3.6 and 55 K. As revealed by the powder refinement (Table I), the smaller lattice parameters and Mn-O-Mn bonding angles are consistent with the evolution of ionic size of the rare-earth atoms.[17,21] Below 42 K, additional peaks appear at 2θ angles which are not allowed in the *Pbnm* symmetry. This reveals the appearance of ICM magnetic fluctuations consistent with the anomalies present in $\varepsilon(T)$, $M(T)$, and $C_p(T)$. As temperature is further lowered, the corresponding magnetic peaks move slightly. At 3.6 K, strong magnetic peaks become evident at several positions [inset of Fig. 2(a)]. We find that the magnetic modulation is along the crystalline b axis with the propagation wave vector q_m

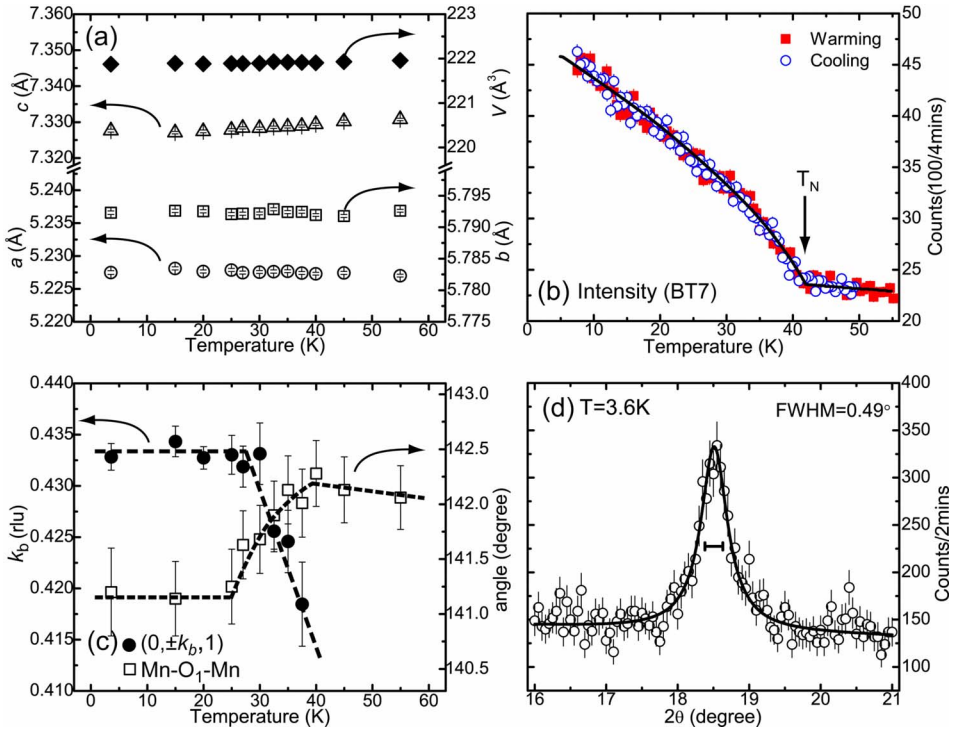

FIG. 3. (Color online) Temperature dependence of (a) the lattice parameters a, b, c, and cell volume V, (b) the peak intensity of $q=(0,\pm k_b,1)$, and (c) the k_b component of the propagation wave vector and the Mn-O_1-Mn bonding angle. (d) The scattering profile near $q=(0,\pm k_b,1)$ at $T=3.6$ K.

$=(0,k_b,0)$. The magnetic satellite peaks occur near the nuclear Bragg peaks (h,k,l) with observed reflection conditions of $h+k=2n$ and $l=2n+1$. The indexing of the magnetic peaks agrees with previous neutron diffraction results of the orthorhombic $YMnO_3$.[26,20] The peaks located at 18.60°, 30.67°, and 51.04° correspond to the reflections from $(0,\pm k_b,1)$, $(1,1-k_b,1)$, $(0,\pm k_b,3)$, and $(2,\pm k_b,1)$.

Figures 3(a)–3(c) summarize the thermal evolution of the structural and magnetic properties derived from the NPD analysis. The crystal structure remains orthorhombic throughout the entire measured temperature range [Fig. 3(a)]. The lattice parameters and cell volume show smooth variations. The typical lattice distortion across the transition due to the magnetoelastic coupling observed in many magnetically frustrated system is less evident.[22,23] However, a sudden collapse in bonding angle of Mn-O_1-Mn (along the c axis) near T_{N1} does indicate the onset of AF order with 180° phase flipping in that direction, while the in-plane Mn-O_2-Mn angle shows no sign of AF correlation near T_{N1}. Figure 3(b) displays the order parameter measured by monitoring the peak intensity at $2\theta=18.6°$, the corresponding wave vector of the strongest magnetic peaks at $(0,\pm k_b,1)$. The intensity increases below T_{N1} with little hysteresis upon cooling and warming. Figure 3(c) plots the T dependence of the magnetic modulation. The wave vector occurs at $(0,k_b,0)$ with $k_b\approx 0.415$ just below T_{N1}, and gradually shifts to a larger value with decreasing temperature. It locks onto $k_b=0.433$ at $T_{N2}=28$ K and remains constant at low temperature. The evolution of the magnetic modulation bears a close resemblance to that of the orthorhombic $YMnO_3$,[20] in which the ICM magnetic order locks onto a wave vector with $k_b=0.435$ below 28 K.[24] Although the magnetic phase transition of $ErMnO_3$ is manifested by the sharp anomaly near T_{N1} in the thermodynamics measurements, the magnetic correlation length remains finite even at the lowest temperature. As shown in Fig. 3(d), the magnetic peaks at $(0,\pm k_b,1)$ and higher scattering angles have Lorentzian profiles indicative of short-range order. The magnetic correlation length ξ is estimated using the method described in Ref. 25:

$$\xi = \pi/\sqrt{2\ln 2}\sigma(q_0), \tag{1}$$

where $\sigma(q_0)$ is the intrinsic width of the magnetic peak with q_0 in units of $Å^{-1}$. We obtain $\xi\approx 210$ Å, much shorter than the instrumental resolution of 1000 Å.

It was initially proposed that $YMnO_3$ forms a helical spin structure with Mn moments within the ac plane and the rotation axis along the b direction.[26] Later neutron diffraction measurements suggest that the Mn spins are sinusoidally modulated, with both the moment direction and modulation wave vector along the b axis in the $Pbnm$ space group.[20] For $ErMnO_3$, it is difficult to definitively determine the magnetic structure, given the short-range nature of magnetic order and limited number of magnetic peaks. Nevertheless, the similar propagation wave vector and T dependence of the modulation wave vector suggest that both $ErMnO_3$ and $YMnO_3$ have the same magnetic structure.

It is interesting to compare the magnetic and ferroelectric properties of three rare-earth perovskite manganites $RMnO_3$ (R=Ho, Y, and Er). Neutron diffraction measurements show that $HoMnO_3$ possesses an E-type magnetic structure[27,28] which is verified theoretically to be stable at low

temperature.[29] The fact that both $HoMnO_3$ and $YMnO_3$ exhibit spontaneous electric polarization at the magnetic lock-in transitions into either commensurate *E*-type or ICM magnetic order strongly indicates a close interplay between the magnetism and ferroelectricity. According to Sergienko *et al.*, the cooperative movement of oxygen atoms resulting from the competition between elastic energy (favoring a distorted Mn-O-Mn bonding angle) and energy gain by the virtual hopping of e_g electrons within the ferromagnetic chain (favoring 180° bonding angle) leads to polarization *P* perpendicular to the magnetic modulations. In $YMnO_3$, the virtual hopping mechanism may still give rise to a local polarization within one ferromagnetic chain but due to the ICM modulation along the *b* axis this polarization will be modulated and reverse sign with the magnetic modulation. The origin of the observed macroscopic polarization in $YMnO_3$ is not yet explained and still a matter of discussion. In the case of $ErMnO_3$, the lack of long-range magnetic correlation (with magnetic domain size around 200 Å) significantly affects the ferroelectric properties. Our preliminary measurements of the pyroelectric current have not been able to prove the existence of a spontaneous polarization above the resolution of the measurement. The weakness of macroscopic polarization is likely linked to the absence of long-range magnetic order. One possible explanation of the magnetic fluctuations is the enhanced magnetic frustration in $ErMnO_3$. We notice considerable increase of Jahn-Teller distortion in the perovskite $RMnO_3$ with small *R* ionic size.[18] The in-plane bonding angle of Mn-O_2-Mn decreases from 144.1° ($HoMnO_3$) and 144.6° ($YMnO_3$) to 143.9° for $ErMnO_3$.[21] Such distortion effectively increases the magnetic frustration due to the competition between the nearest-neighbor FM interaction and the next-nearest-neighbor AFM interaction in the *ab* plane.[30] The short-range magnetic order of Mn spins could also be related to the paramagnetic Er^{3+} ions in that temperature range. These paramagnetic fluctuations might not be sufficient to support the long-range magnetic order at the Mn sites. The contribution of the rare-earth magnetic moment is further emphasized in $HoMnO_3$. The strong external field dependence of the ferroelectric polarization in that material reveals the active role of the holmium moment order in stabilizing the magnetic structure and enhancing of the FE. A similar feature has been reported in the multiferroic perovskite $DyMnO_3$,[31] where the ICM order of Dy moments closely tracks the evolution of the FE polarization and suppresses it when the Dy moment becomes commensurate.

In summary, we have used dielectric, magnetization, and specific heat measurements as well as high-resolution neutron powder diffraction to investigate the thermodynamic and magnetic properties of the orthorhombic perovskite $ErMnO_3$. The system forms ICM AF correlation below 42 K and undergoes a lock-in transition at 28 K with propagation wave vector of (0,0.433,0). The magnetic fluctuations remain short-range at low *T*. The correlation of the magnetic and ferroelectric properties is also discussed.

We thank I. Sergienko for useful discussions. Oak Ridge National Laboratory is managed by UT-Battelle, LLC, for the U.S. Department of Energy under Contract No. DE-AC05-00OR22725. The work is supported by the U.S. DOE BES under Contract No. DE-FG02-05ER46202, the T.L.L. Temple Foundation, the J. J. and R. Moores Endowment, and the State of Texas through TCSUH.

*yef1@ornl.gov

[1] T. Kimura *et al.*, Nature (London) **426**, 55 (2003).
[2] N. Hur *et al.*, Nature (London) **429**, 392 (2004).
[3] G. Lawes *et al.*, Phys. Rev. Lett. **95**, 087205 (2005).
[4] N. Ikeda *et al.*, Nature (London) **436**, 1136 (2005).
[5] T. Kimura, J. C. Lashley, and A. P. Ramirez, Phys. Rev. B **73**, 220401(R) (2006).
[6] K. Taniguchi *et al.*, Phys. Rev. Lett. **97**, 097203 (2006).
[7] Y. Yamasaki *et al.*, Phys. Rev. Lett. **98**, 147204 (2007).
[8] D. I. Khomskii, J. Magn. Magn. Mater. **306**, 1 (2006).
[9] W. Eerenstein, N. D. Mathur, and J. F. Scott, Nature (London) **442**, 759 (2006).
[10] S.-W. Cheong and M. Mostovoy, Nat. Mater. **6**, 13 (2007).
[11] H. Katsura, N. Nagaosa, and A. V. Balatsky, Phys. Rev. Lett. **95**, 057205 (2005).
[12] I. A. Sergienko and E. Dagotto, Phys. Rev. B **73**, 094434 (2006).
[13] M. Mostovoy, Phys. Rev. Lett. **96**, 067601 (2006).
[14] I. A. Sergienko, C. Sen, and E. Dagotto, Phys. Rev. Lett. **97**, 227204 (2007).
[15] B. Lorenz, Y. Q. Wang, Y. Y. Sun, and C. W. Chu, Phys. Rev. B **70**, 212412 (2004).
[16] B. Lorenz, Y. Q. Wang, and C. W. Chu, arXiv:cond-mat/0608195 (unpublished).
[17] J.-S. Zhou *et al.*, Phys. Rev. B **74**, 014422 (2006).
[18] M. Tachibana *et al.*, Phys. Rev. B **75**, 144425 (2007).
[19] J. Kim *et al.*, Phys. Rev. B **74**, 052406 (2006).
[20] A. Muñoz *et al.*, J. Phys.: Condens. Matter **14**, 3285 (2002).
[21] J. A. Alonso *et al.*, Inorg. Chem. **39**, 917 (2000).
[22] L. C. Chapon *et al.*, Phys. Rev. Lett. **93**, 177402 (2004).
[23] F. Ye *et al.*, Phys. Rev. B **73**, 220404(R) (2006).
[24] An accurate determination of the propagation wave vector $(0,k_b,0)$ is difficult even below the "lock-in" transition. However, the similar magnetic behavior between $ErMnO_3$ and $YMnO_3$ indicates that the magnetic structure of $ErMnO_3$ at low temperature is also incommensurate.
[25] Harold P. Klug and Leroy E. Alexander, *X-ray Diffraction Procedures: For Polycrystalline and Amorphous Materials* (John Wiley & Sons, New York, 1974).
[26] S. Quezel, J. Rossat-Mignod, and E. F. Bertaut, Solid State Commun. **14**, 941 (1974).
[27] A. Muñoz *et al.*, Inorg. Chem. **40**, 1020 (2001).
[28] H. W. Brinks *et al.*, Phys. Rev. B **63**, 094411 (2001).
[29] S. Picozzi, K. Yamauchi, G. Bihlmayer, and S. Blügel, Phys. Rev. B **74**, 094402 (2006).
[30] T. Kimura *et al.*, Phys. Rev. B **68**, 060403(R) (2003).
[31] O. Prokhnenko *et al.*, Phys. Rev. Lett. **98**, 057206 (2007).